WILEY Applied Organometallic Chemistry

A new strategy to design a graphene oxide supported palladium complex as a new heterogeneous nanocatalyst and application in carbon–carbon and carbon-heteroatom cross-coupling reactions

Kiumars Bahrami[1,2] (ID) | Homa Targhan[1]

[1] Department of Organic Chemistry, Faculty of Chemistry, Razi University, Kermanshah 67149-67346, Iran

[2] Nanoscience and Nanotechnology Research Center (NNRC), Razi University, Kermanshah 67149-67346, Iran

Correspondence
Kiumars Bahrami, Nanoscience and Nanotechnology Research Center (NNRC), Razi University, Kermanshah, 67149-67346, Iran.
Email: kbahrami2@hotmail.com

The palladium nanoparticles were successfully stabilized with an average diameter of 6–7 nm through the coordination of palladium and terpyridine-based ligands grafted on graphene oxide surface. The graphene oxide supported palladium nanoparticles were thoroughly characterized and applied as an efficient heterogeneous catalyst in carbon–carbon (Suzuki-Miyaura, Mizoroki-Heck coupling reactions) and carbon–heteroatom (C-N and C-O) bond-forming reactions. The catalyst was simply recycled from the reaction mixture and was reused consecutive four times with small drop in catalytic activity.

KEYWORDS
cross-coupling, graphene oxide, heterogeneous nanocatalyst, palladium-catalyzed, terpyridine-based ligands

1 | INTRODUCTION

Cross-coupling reactions have found widespread use in the creation of carbon–carbon (Suzuki–Miyaura, Kumada–Corriu, Stille, Mizoroki–Heck, Sonogashira, Hiyama and Negishi reactions) and carbon–heteroatom (C-O, C-N and C-S) bonds[1] and always get prior importance in the field of synthetic organic chemistry as well as in medicinal chemistry.[2,3] It should be noted that progress on cross-coupling reactions plays an important role in the development of pharmaceutical industry. These reactions provide new roads for design and preparation of drug substances.[4] For example, the cross-coupling reactions are considered as key steps in production of Losartan®,[5] Zyprexa,[6] Singulair,[7] (+)-Dynemicin,[8] Morphine[9] and Paclitaxel.[10] The importance of scientific advances associated with cross-coupling was demonstrated by awarding Richard F. Heck, Ei-ichi Negishi and Akira Suzuki the Nobel Prize in chemistry in 2010 for the development of palladium-catalyzed cross coupling.[2,11]

Palladium catalysts are well known for the carbon–carbon and carbon–heteroatom bonds formation in reactions of aryl halides via cross-coupling reactions on both academic and industrial scales.[12] During the last few decades, major advances in homogeneous palladium-catalyzed coupling reactions have been described by a number of research groups.[2] Considering the extensive use of palladium in cross-coupling reactions and high cost and toxicity of palladium on the other hand, there is a growing interest in applying heterogeneous and recoverable palladium catalysts, therefore the heterogenization of palladium catalysts is extremely important from both environmentally and economic points of view.[13–19]

Recent developments in nanotechnology has significantly improved catalyst performance.[20] Nano-sized catalysts have high surface area thereby increase the contact between reactants and catalyst and speed up the catalytic process. In other hand, due to insolubility in reaction solvents, nanocatalysts are easily separated from the reaction mixture and are reusable systems. In addition, researchers

have shown that activity and selectivity of nanocatalysts can be controlled by tailoring chemical and physical properties of nanocatalysts including particle size and surface composition, shape and morphology via techniques for preparing nanocatalysts.[21] It is well known that particle size of metals strongly impacted their catalytic properties, a decrease in particle size increases the surface area the number of edge and corner atoms and these lead to the improvement of the catalytic properties of metals. Therefore, metal particles must be generated as small as possible. For this purpose and stabilization of metal nanoparticles, different types of stabilizers, such as surfactants, polymers, and dendrimers, micelles and various ligands as well as anchoring of metal particles on supports are presented.[22] In the last decade, metal nanoparticles supported on high-surface-area solid carriers such as porous silica, alumina, zeolites, Fe_3O_4 and other oxides, mesoporous materials, carbon nanofibers, multi-walled carbon nanotubes, hollow carbon nanospheres, graphene oxide etc. have been prepared and employed as catalysts.[23,24]

Graphene oxide (GO) is a two-dimensional carbon sheet decorated with oxygenated functional groups, such as hydroxyl (OH), carbonyl (C=O) and alkoxy (C–O–C) groups, which is prepared from oxidation of graphite.[25,26] GO is commonly produced by the oxidative treatment of graphite with $KMnO_4$ and $NaNO_3$ in concentrated H_2SO_4 via Hummers method as a reliable method.[27] The peculiar properties of graphene oxide such as easy dispersibility in many solvents and particularly in water,[28] low cost,[29] electronic, optical, thermal, mechanical, and electrochemical properties, as well as chemical reactivity and high surface area[30] make it as a good candidate for application in electronic and energy storage devices, biosensors, coating agents, water purification machine and as a support material for the synthesis of heterogeneous catalysts.[26,31]

Inspiring from recent developments in the field of nanocatalyst, herein, we report preparation and characterization of GO-supported palladium complex with two types of 2,2′: 6′,2″-terpyridine ligands (4′-(4-hydroxyphenyl)-2,2′:6′,2″-terpyridine (HPTPy) and 1,4-Bis(2,2′: 6′,2″-terpyridin-4′-yl)benzene (TPy-C_6H_4-TPy)) which

has also been applied as nanocatalyst for the C − C, C − N and C-O bond formations via cross-coupling reactions of aryl halides.

The terpyridines were first discovered by Morgan and Burstall in 1932, from the reaction of pyridine with $FeCl_3$.[32] The terpyridine derivatives consist of three pyridine rings and because of efficient and stable chelating ability to transition metals, are used as multidentate polypyridine ligands to prepare coordination complexes.[33–35]

The GO-supported palladium TPy complex [denoted as (1,4-C_6H_4)(GO-CPTMS@HPTPy-Pd-TPy)$_2$] was facilely prepared through a simple process and applied as an effective and reusable catalyst to create carbon–carbon bond via Suzuki-Miyaura, Mizoroki-Heck and carbon–heteroatom (C-O, C-N) bonds (Scheme 1).

2 | RESULTS AND DISCUSSION

2.1 | Catalyst characterization

The stages of (1,4-C_6H_4)(GO-CPTMS@HPTPy-Pd-TPy)$_2$ preparation are summarized in Scheme 2. Initially, the graphene oxide is typically prepared employing modified Hummers method[27,36] and modified by using CPTMS,[26] then HPTPy ligand (see Supporting Information), prepared according to the literature reports,[35,37] connected to GO-CPTMS. Subsequent, the process for preparing the catalyst is complete with added TPy-C_6H_4-TPy, synthesized according to Vaduvescu and Potvin report,[38] and $PdCl_2$.

The prepared catalyst was extensively analyzed through some characterization techniques including Fourier transform infrared spectroscopy (FT-IR), transmission electron microscopy (TEM), scanning electron microscopy (SEM), thermogravimetric analysis (TGA), energy-dispersive X-ray spectroscopy (EDX), X-ray diffraction spectroscopy (XRD), UV–Vis spectra analysis and inductively coupled plasma (ICP).
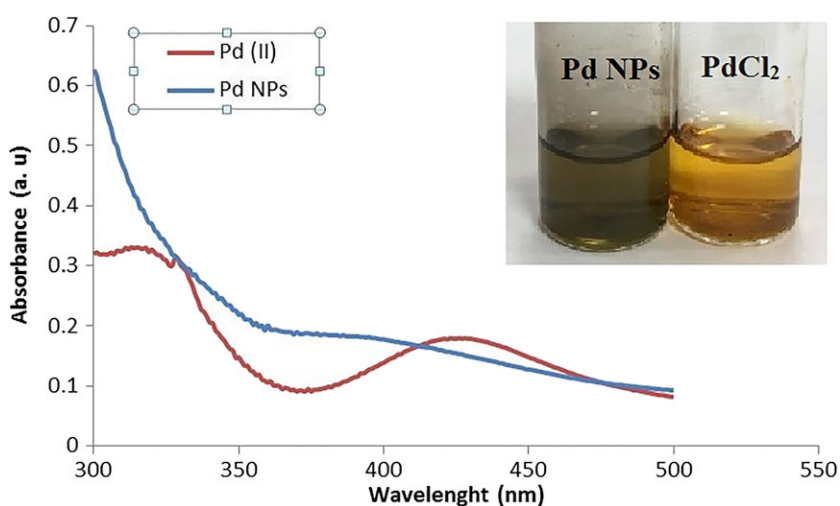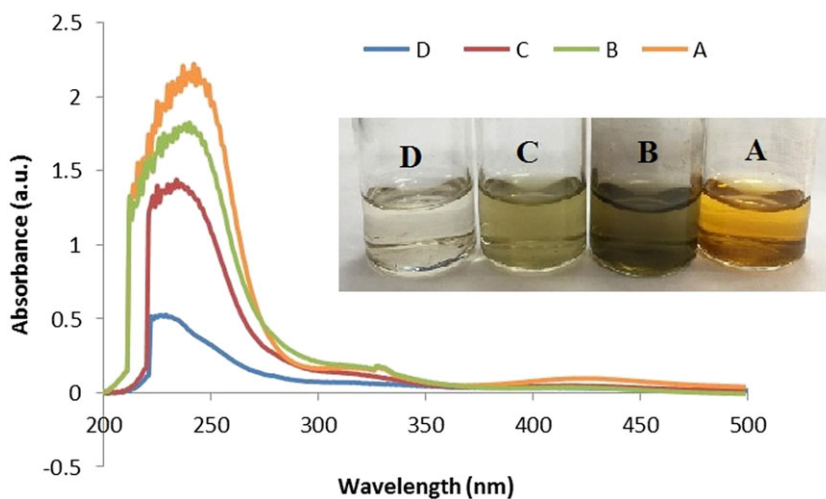
Conversion of $PdCl_2$ to Pd NPs using EtOH as reducing agent has been well documented and recognized.[39,40] In this regard, the synthesis of the Pd(0)
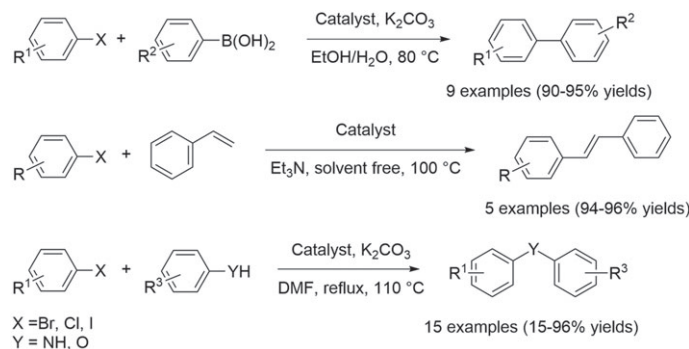

SCHEME 1 GO supported Pd nanoparticles catalyzed C-C, C-N and C-O bonds-forming reactions
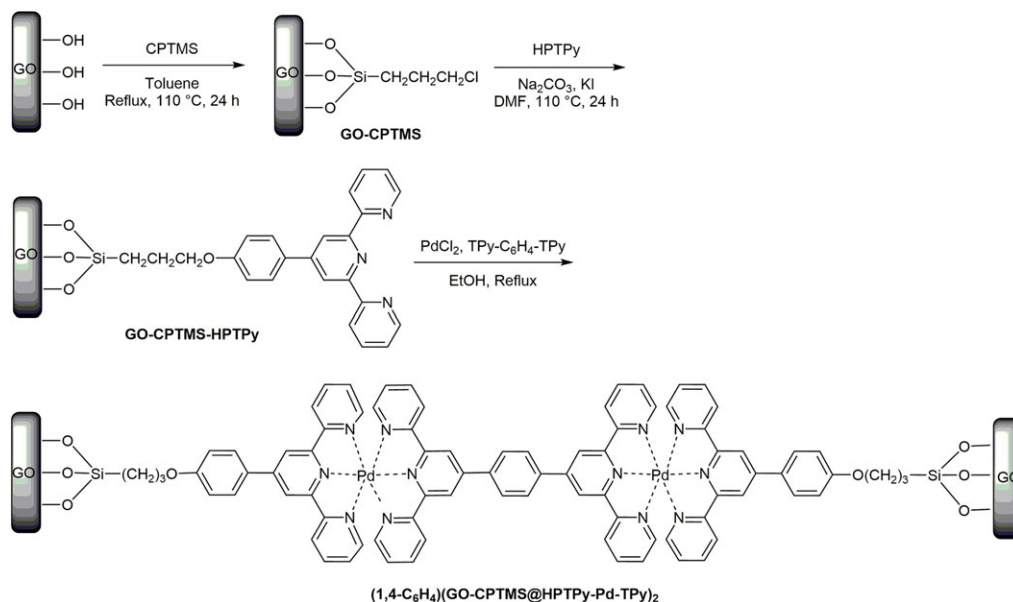
SCHEME 2 Synthesis steps of the catalyst

FIGURE 1 UV–visible spectra of PdCl$_2$ solution and Pd NPs

FIGURE 2 Representative UV–Vis spectra of soluble PdCl$_2$ in EtOH (A), PdCl$_2$ and GO-CPTMS in EtOH (B) and mixtures of PdCl$_2$ and GO-CPTMS@TPy in EtOH in the absence and presence of the TPy-C$_6$H$_4$-TPy (C and D respectively) monitored at 24 hr. The solution was refluxed at 80 °C and spectra are recorded at 30 °C
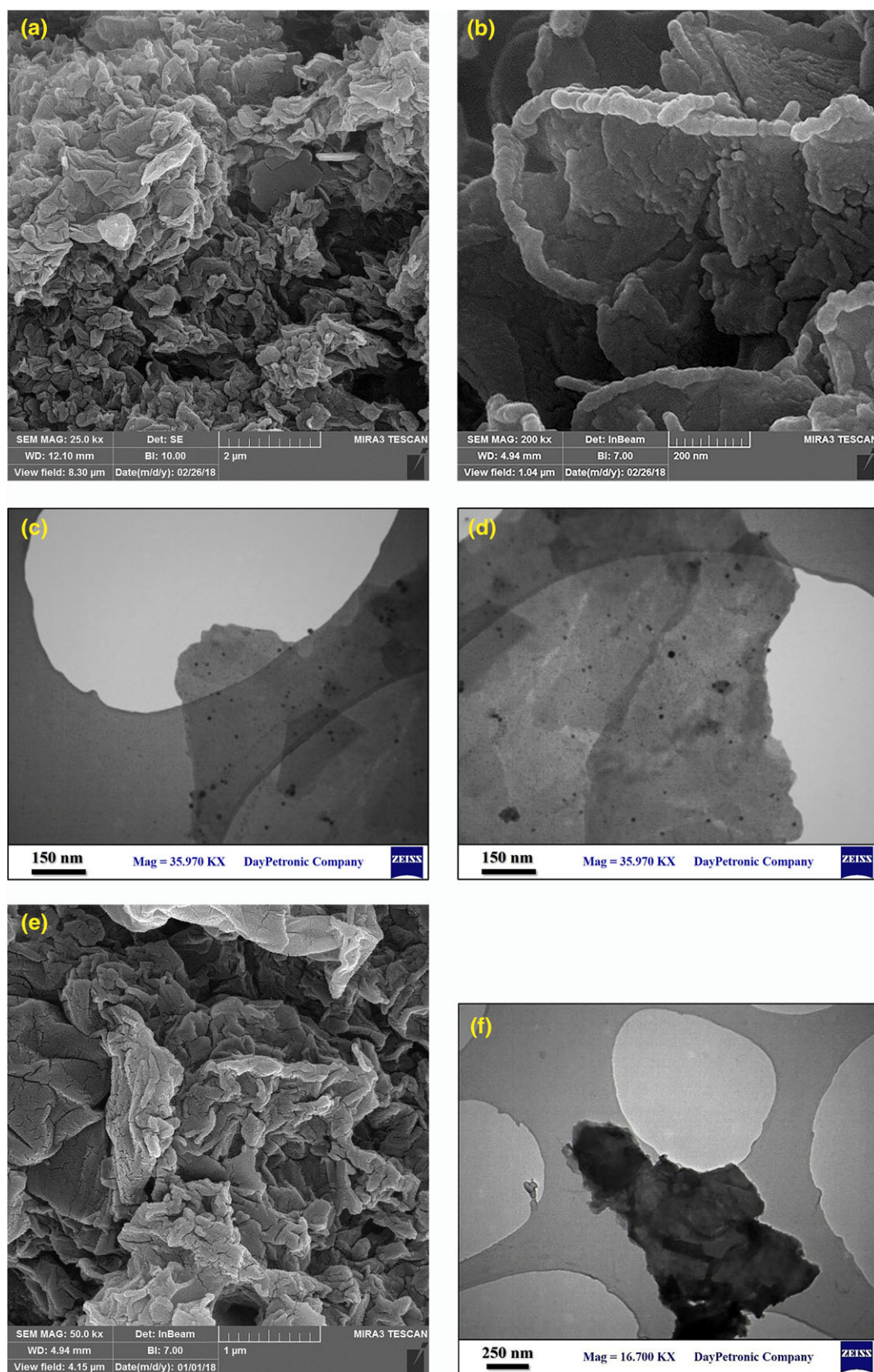
FIGURE 3 (a) and (b) SEM images, (c) and (d) TEM images of $(1,4\text{-}C_6H_4)(GO\text{-}CPTMS@HPTPy\text{-}Pd\text{-}TPy)_2$, (e) SEM image (f) TEM image of GO

catalyst was initially monitored by UV–Visible spectroscopy (Figure 1). In UV–visible spectroscopy, the $PdCl_2$ solution showed a distinct peak approximately at 425 nm indicating the existence of Pd (II) ion. During the formation of Pd NPs on the GO-CPTMS@-terpyridine-based ligands, the UV–Vis spectrum showed conversion of Pd (II) to Pd(0) by the absence of the peak at 425 nm. The formation of Pd(0) nanoparticles was also confirmed by the color change of palladium solution from yellowish into dark brown during the catalyst synthesis within 24 hr (Figure 1).[13,41,42]

As mentioned in leterature, in the case of noble metals, one of the most widely used methods to stabilize the nanoparticles and control their growth is to use ligands[43] and it is observed that tridentate nitrogen ligands, including terpyridine-based ligands, increase the dispersion and stability of the metal nanoparticles due to the strong interaction metal-nitrogen and the formation of two five-membered metallacycles.[44,45]

Furthermore, the reduction of Pd (II) ions and the stabilization of Pd NPs on GO-CPTMS and GO-CPTMS@-TPy in the presence and absence of the TPy-Ph-TPy was monitored by the UV–Vis spectra analysis in the presence of EtOH as green solvent and reducing agent. Figure 2 shows UV–Vis spectra of soluble $PdCl_2$ in EtOH (A), $PdCl_2$ and GO-CPTMS in EtOH (B) and mixtures of $PdCl_2$ and GO-CPTMS@TPy in EtOH in the absence and presence of the TPy-Ph-TPy (C and D respectively), in $PdCl_2$ and GO-CPTMS@TPy sample, the intensity at 240 nm is decreased more than the case of GO-CPTMS after 24 hr which indicates the more stabilization of Pd NPs on GO-CPTMS@TPy (C). The peak of 245 nm began to

disappear in the presence of the TPy-C_6H_4-TPy, which showed significant increase in stabilization of Pd NPs on GO-CPTMS@TPy was observed after 24 hr (D). As was expected, TPy and TPy-Ph-TPy ligands can act as effective stabilizers for Pd species.

Figures 3a and 3b display SEM images (1,4-C_6H_4)(GO-CPTMS@HPTPy-Pd-TPy)$_2$ with different magnifications. TEM images of the prepared nanocatalyst are shown in Figures 3c and 3d. It can be seen that uniform and small sized Pd nanoparticles, with 6–7 nm average diameters, have been dispersed on surface of GO layers. Figures 3e and 3f also show SEM and TEM images of Go, respectively.
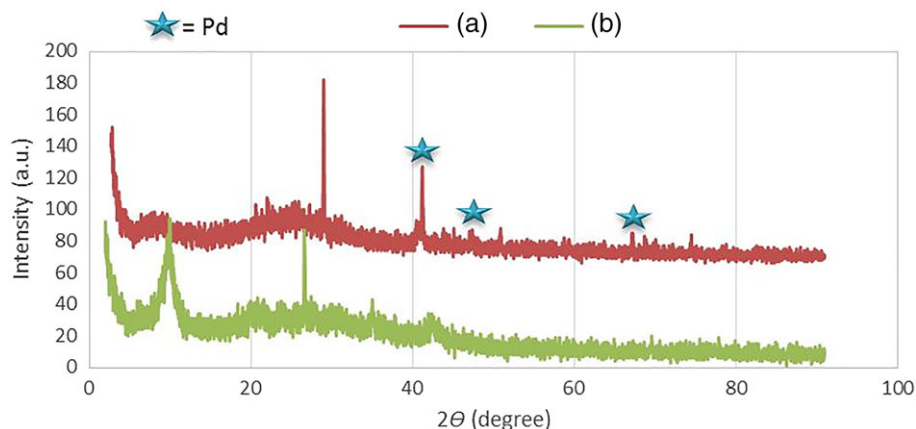
EDX technique can be used for the elemental analysis of the nanocatalyst, therefore successful functionalization of the GO can be inferred from this technique. EDS spectrum shows the presence of C, Si, O, N and Pd in the structure of (1,4-C_6H_4)(GO-CPTMS@HPTPy-Pd-TPy)$_2$ (Figure 4).

Figure 5 presents XRD patterns of the synthesized graphene oxide and (1,4-C_6H_4)(GO-CPTMS@HPTPy-Pd-TPy)$_2$. The diffraction peaks at the Bragg angles of 41.1°, 46.7°, and 68.2° correspond to the 111, 200, and 220 facets of elemental palladium.[46,47]

FT-IR technique can also be used to track the synthesis and modification of GO and connection of HPTPy on the surface of modified graphene oxide (Figure 6). In the FT-IR spectrum of GO, following functional groups were identified: OH stretching vibrations (3424 cm^{-1}), C=O stretching vibration (1729 cm^{-1}), C=C from unoxidized sp^2 CC bonds (1414, 1627 cm^{-1}), and CO vibrations (1225 cm^{-1}). In the case of GO-CPTMS, the sharp band at 1037 cm^{-1} corresponds to Si–O–Si antisymmetric

Element	W%	A%
C	34.38	52.58
N	6.97	9.15
O	16.14	18.53
Si	25.77	16.86
Pd	16.73	2.89
	100.00	100.00
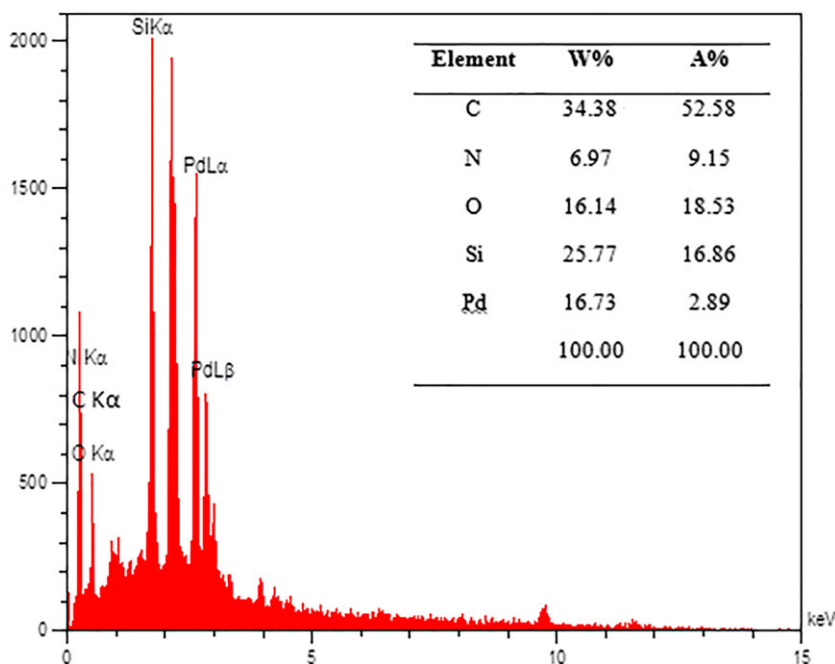
FIGURE 4 EDX pattern of (1,4-C_6H_4)(GO-CPTMS@HPTPy-Pd-TPy)$_2$

FIGURE 5 (a) XRD patterns of $(1,4\text{-}C_6H_4)(\text{GO-CPTMS@HPTPy-Pd-TPy})_2$ and (b) GO
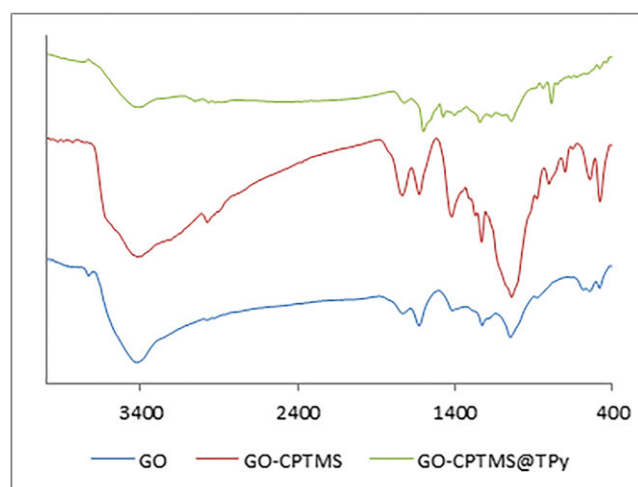
FIGURE 6 FT-IR spectra of GO, GO-CPTMS and GO-CPTMS@TPy

stretching. The peak appearing at 799 cm^{-1} is due to thesymmetric vibration of Si–O–Si. The weak absorption in 2975 cm^{-1} is attributed to the sp^3 C-H stretching vibrations. When the HPTPy was connected on the GO-CPTMS surface, the band observed at 1598 cm^{-1} can be attributed to the C=N stretching frequency. The weak sp^2 C-H stretching vibration of aromatic rings is appeared in 3052 cm^{-1}.

The thermal behaviour of the nanocatalyst was investigated by thermogravimetric analysis (TGA). According to literature graphene oxide tends to lose up to ~50% of its weight between 150 and 350 °C. This is an irreversible effect caused by the detachment of labile oxygen-containing functional groups located on GO support.[48] The weight loss in this temperature range for our nanocatalyst is 9.84%, which indicates that the most oxygen carrying functionalities from GO surface were utilized in Si-O bond formation between GO and CPTMS. A weight loss of 10.14% is observed from 350 to 500 °C,

which is ascribed to the thermal decomposition of organic compounds from nanocatalyst surface (Figure 7).

2.2 | Catalytic studies

The catalytic activity of the prepared GO supported nanocatalyst was evaluated in the carbon–carbon (Suzuki–Miyaura, Mizoroki–Heck reactions) and carbon–heteroatom (C-O, C-N) bonds formation *via* cross coupling reactions. Initially, for the optimization of the Suzuki C-C coupling reaction, a reaction of iodobenzene with phenylboronic acid under different reaction conditions such as different temperatures, solvents, bases and in the presence of various amounts of catalyst was examined as a model reaction. The best result (95% yield) was obtained by using iodobenzene (1.2 mmol), phenylboronic acid (1 mmol) and K$_2$CO$_3$ (1.5 mmol) in the presence of the catalyst (0.01 gr, 1.38 mol%) in a mixture of EtOH/H$_2$O (2/1) at 80 °C (Table 1, entry 3). To show the necessity of terpyridine ligand in this catalyst, we run a control experiment with GO-CPTMS-Pd as a catalyst without the terpyridine attachment (Table 1, entry 4). As can be seen, the reaction produces lower yield of product.

Under these optimized conditions, the generality and scope of the procedure was assessed in the reaction of substituted aryl halides with arylboronic acids and the results are summarized in Table 2. As shown in Table 2, the coupling reaction between aryl halides containing electron-donating groups (Table 2, entry 8) as well as electron withdrawing groups (Table 2, entries 2, 4) with arylboronic acids performed to afford corresponding biaryl products in good to excellent yields. As expected, the Suzuki reaction of aryl chlorides required longer reaction times, because aryl chlorides are generally less reactive toward aryl bromides and iodides.
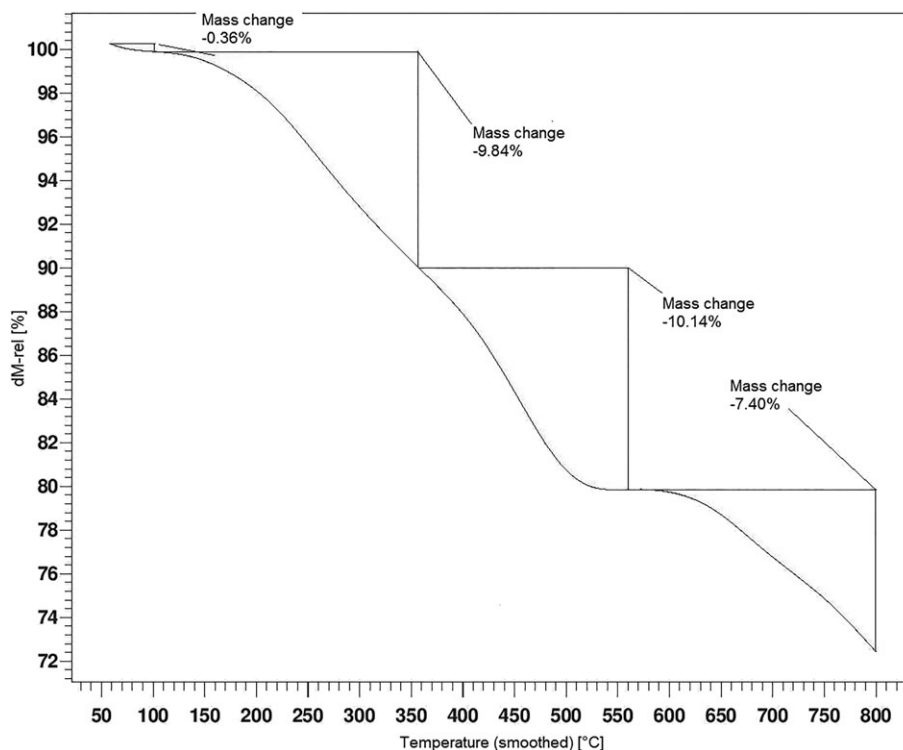
FIGURE 7 TGA curve of (1,4-C$_6$H$_4$)(GO-CPTMS@HPTPy-Pd-TPy)$_2$

TABLE 1 Optimization of conditions in the Suzuki-Miyaura coupling reaction[a]

Entry	Catalyst	Base	Solvent	T (°C)	Yield (%)[b]
1	0.69 mol%	K$_2$CO$_3$	EtOH/H$_2$O (2/1)	80	35
2	1.10 mol%	K$_2$CO$_3$	EtOH/H$_2$O (2/1)	80	75
3	1.38 mol%	K$_2$CO$_3$	EtOH/H$_2$O (2/1)	80	95
4	0.01 gr[c]	K$_2$CO$_3$	EtOH/H$_2$O (2/1)	80	35
5	1.38 mol%	K$_2$CO$_3$	DMF	80	96
6	1.38 mol%	K$_2$CO$_3$	H$_2$O	80	20
7	1.38 mol%	NEt$_3$	EtOH/H$_2$O (2/1)	80	50
8	1.38 mol%	K$_2$CO$_3$	EtOH/H$_2$O (2/1)	r.t.	20

[a]Reaction conditions: Iodobenzene (1.2 mmol), phenylboronic acid (1 mmol), base (1.5 mmol), solvent (3 mL), under air atmosphere, 3 hr.
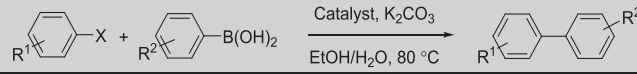
[b]Isolated yields.

[c]Catalyst: GO-CPTMS-Pd.

In a subsequent step, we investigated the catalytic activity of (1,4-C$_6$H$_4$)(GO-CPTMS@HPTPy-Pd-TPy)$_2$ for the Mizoroki−Heck C-C coupling reaction. The bromobenzene (1 mmol) and styrene (1.2 mmol) were selected as substrates to establish the best condition for the preparation of the corresponding trans-stilbenes in the presence of different amount of the catalyst and various bases and solvents at 100 °C. Initially, the reaction was performed in the absence of catalyst and no product
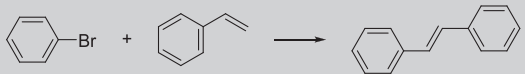
obtained. After careful examinations, the use of 0.01 gr (1.38 mol%) of the catalyst in the presence of Et$_3$N (3 mmol) as a base under solvent-free conditions at 100 °C was found to be the optimal condition for the synthesis of trans-stilbenes (Table 3, entry 4). In Table 4 are reported the results for the coupling of styrene with aryl halides using the Pd nanocatalyst and forming corresponding trans-stilbenes in the optimal conditions. As Table 4 shows, donor- and acceptor substituted aryl

TABLE 2 Suzuki−Miyaura coupling reactions of aryl halides with phenylboronicacid[a]

$$R^1 \text{-}\!\!\!\diagdown\!\!\!\diagup\text{-}X \; + \; R^2 \text{-}\!\!\!\diagdown\!\!\!\diagup\text{-}B(OH)_2 \xrightarrow[\text{EtOH/H}_2\text{O, 80 °C}]{\text{Catalyst, K}_2\text{CO}_3} R^1 \text{-}\!\!\!\diagdown\!\!\!\diagup\text{-}\!\!\!\diagdown\!\!\!\diagup\text{-}R^2$$

Entry	X	R¹	R²	Time (h)	Yield (%)[b]	TOF (h⁻¹)	Mp[Ref.]
1	I	H	H	3	95	23.19	66[49]
2	I	4-NO₂	H	3	92	22.22	114[50]
3	I	H	4-CH₃	3	98	23.67	42–44[50]
4	I	4-NO₂	3-NO₂	3	95	23.19	180–184[51]
5	Br	H	H	3	92	22.22	65–67[49]
6	Br	H	4-OCH₃	3	93	22.46	85–88[50]
7	Br	H	4-F	3	95	23.19	74–76[52]
8	Br	4-CH₃	H	3	95	23.19	45[50]
9	Cl	H	H	5	90	13.04	65[49]

[a]Reaction conditions: Iodobenzene (1.2 mmol), phenylboronic acid (1 mmol), catalyst (1.38 mol%), base (1.5 mmol), solvent (3 mL), under air atmosphere.
[b]Isolated yields.

TABLE 3 Optimization of reaction conditions[a]

$$\text{Ph-Br} + \text{styrene} \longrightarrow \text{stilbene}$$

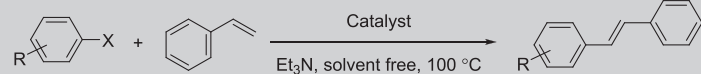| Entry	Catalyst (mol%)	Base	Solvent	Yield(%)[b]
1	No catalyst	NEt₃	No solvent	0
2	0.69	NEt₃	No solvent	35
3	1.10	NEt₃	No solvent	70
4	1.38	NEt₃	No solvent	92
5	1.38	K₂CO₃	DMF	92

[a]Reaction conditions: bromobenzene (1 mmol), styrene (1.2 mmol), base (3 mmol), solvent (3 mL), at 100 °C, under air atmosphere, 4 hr.
[b]Isolated yields.

bromides and iodides have been reacted with styrene in mostly excellent yields, however, aryl bromides require longer reaction times.

As an extension to use of the GO-supported palladium complex, we also employed this nanocatalyst for arylation of amines and phenols with aryl halides. The reaction of iodobenzene (1.2 mmol) with aniline (1 mmol) was first studied as standard substrate with the prepared nanocatalyst (Table 5). We found that the reaction occurred to afford diphenylamine in 92% yield when it was stirred for 24 hr at 100 °C in the presence of 0.01 gr (1.38 mol%) (1,4-C₆H₄)(GO-CPTMS@HPTPy-Pd-TPy)₂ and 3 mmol of K₂CO₃ in DMF under air (Table 5 entry 2).

In order to study the generality of this procedure, the reaction of other amines and substituted phenols were next studied. As shown in Table 6, electron-rich, −neutral, and -poor substituted anilines are all converted to secondary aromatic amines by reaction with iodobenzene in the yield ranging from 85 to 92%. Secondary amines, e.g., diphenylamine (yield 50%), do not exhibit as high yields as primary amines. When iodobenzene was replaced by
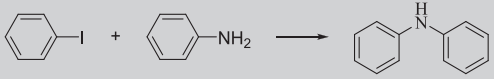
TABLE 4 Coupling reactions of aryl halides with styrene[a]

$$R\text{-}\!\!\!\diagdown\!\!\!\diagup\text{-}X \; + \; \text{styrene} \xrightarrow[\text{Et}_3\text{N, solvent free, 100 °C}]{\text{Catalyst}} R\text{-}\!\!\!\diagdown\!\!\!\diagup\text{-}\!\!\!\diagup\!\!\!\diagdown\text{-Ph}$$

Entry	X	R	Time (h)	Yield (%)[b]	TOF (h⁻¹)	Mp[Ref.]
1	I	H	4	95	17.21	115–120[53]
2	I	4-NO₂	4	92	16.67	148–150[53]
3	Br	H	5	92	13.33	112–116[53]
4	Br	4-NO₂	5	90	13.04	150–152[53]
5	Br	4-CH₃	5	90	13.04	116[54]

[a]Reaction conditions: Aryl halide (1 mmol), styrene (1.2 mmol), catalyst (1.38 mol%), NEt₃ (3 mmol), under solvent-free, 100 °C.
[b]Isolated yields.

TABLE 5 Optimization of reaction conditions for arylation of amines and phenols[a]

Entry	Catalyst (mol%)	Base	Solvent	T (°C)	Yield (%)[b]
1	1.10	K_2CO_3	DMF	100	80
2	1.38	K_2CO_3	DMF	100	92
3	1.38	K_2CO_3	Toluene	100	65
4	1.38	K_2CO_3	EtOH	100	60
5	1.38	K_2CO_3	DMF	r.t	trace
6	1.38	K_2CO_3	DMF	60	50
7	1.38	NEt_3	DMF	100	55

[a]Reaction conditions: Iodobenzene (1.2 mmol), aniline (1 mmol), under air atmosphere, 24 hr.
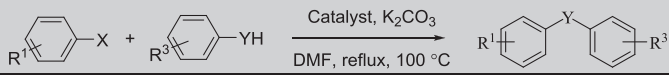
[b]Isolated yields.

bromobenzene, the coupling reaction was not effective. Indeed, the reaction of bromobenzene with aniline occurred in 15% yield (Table 6, entry 6), significantly lower than the reaction of iodobenzene with aniline. This method has been utilized for the creation of C-O bond and provided a number of diaryl ethers in high to excellent yields. In the case of C-O bond formation, bromobenzene is reactive almost as much as iodobenzene. Both hydroxyl groups of the hydroquinone molecule can conceivably react with iodobenzene and 1,4-diphenoxybenzene is synthesized in 92% yield (Table 6, entry 10).

Furthermore, the catalyst easily separated from the reaction mixture by centrifugation and washed two times with ethanol and followed by water, finally dried for the next run. Remarkably, the recovered catalyst still remained highly active and was reused consecutive three times with small drop in catalytic activity. Reusability results confirm that no substantial loss of palladium from the catalyst surface happens during the reactions. To confirm this further, leaching of Pd during the course of the catalytic reactions was examined by ICP analysis. ICP showed 1 gr of the manufactured catalyst and the catalyst after four catalytic cycles, containing 1.38 and 1.22 mmol of Pd, respectively. The results confirmed the chemical stability and reusability of the (1,4-C_6H_4)(GO-CPTMS@HPTPy-Pd-TPy)$_2$ nanocatalyst.

The efficiency of the synthesized catalyst in this work is compared to some graphene oxide supported Pd

TABLE 6 Arylation of amines and phenols

Entry	X	Y	R^1	R^3	Yield (%)[b]	TOF (h^{-1})	Mp[Ref.]
1	I	NH	H	H	92	2.78	53[55]
2	I	NH	4-NO_2	H	85	2.57	130[56]
3	I	NH	H	4-NO_2	90	2.72	129[57]
4	I	NH	H	4-CH_3	85	2.57	85–90[57]
5	I	N-Ph	H	H	50	1.51	124[58]
6	Br	NH	H	H	15	0.45	-
7	I	O	H	H	96	2.90	Oil[59]
8	I	O	4-NO_2	H	93	2.81	56–58[59]
9	I	O	4-NO_2	4-NO_2	90	2.72	145[60]
10	I	O	H	4-OH	92[c]	2.78	75–77[61]
11	I	O	4-NO_2	4-Cl	90	2.72	76[62]
12	I	O	4-NO_2	4-OCH_3	92	2.78	108[63]
13	I	O	4-NO_2	3,5-diMe	92	2.78	74–76[64]
14	Br	O	H	H	88	2.66	Oil[59]
15	Cl	O	H	H	25	0.75	-

[a]Reaction conditions: Iodobenzene (1.2 mmol), amines or substituted phenols (1 mmol), catalyst (1.38 mol%), K_2CO_3 (3 mmol), DMF, 100 °C, under air atmosphere, 24 hr.

[b]Isolated yields.

[c]2.4 mmol of iodobenzene was used.

nanocatalysts in Suzuki and Heck coupling reactions. Table 7 shows that this catalyst is superior to some previously reported nanocatalysts in terms of yields and reaction times.

3 | EXPERIMENTAL

3.1 | Material and physical measurements

The materials were purchased from Merck and Fluka and were used without any additional purification. All reactions were monitored by TLC. Melting points were determined using a Stuart Scientific SMP2 apparatus. FT-IR spectra were determined with a PerkinElmer 683 instrument. ^{1}H NMR and ^{13}C NMR spectra were recorded with a Bruker (250 and 400 MHz) spectrometer in CDCl$_3$ as solvent. TGA was carried out with a STA PT- 1000 Linseis instrument (Germany) under air atmosphere at a heating rate of 10 °C min^{-1}. SEM and energy-dispersive X-ray (EDX) measurements were performed using a TESCAN- MIRA3 operated at 26 kV with the electron gun filament: tungsten. TEM observations were carried out with a Zeiss-EM10C (Germany) operating at 100 kV with samples on formvar carbon-coated grid Cu mesh 300. The elemental palladium content of nanocatalyst was determined by Perkin Elmer Optima 7300D inductively coupled plasma (ICP). X-rays diffraction (XRD) patterns were obtained using STOE STADI-P diffractometer (Cu K-alpha1 radiation wavelength = 1.54060 Å).

3.2 | Synthesis of GO

GO was synthesized employing modified Hummer's method.[27,36] Briefly, concentrated H$_2$SO$_4$ (15 mL) was added to a mixture of graphite (0.3 g) and NaNO$_3$ (0.3 g), and the mixture was cooled to 0 °C in an ice-salt bath. Under stirring, KMnO$_4$ (1.5 g) was added slowly to the suspension over 2 hr at 0 to 10 °C with ice-salt bath cooling. The mixture was warmed to 35 °C and stirred for 30 min, and the resulting solution was diluted by slowly adding 30 mL of water under stirring. Then the reaction was stirred under reflux for 15 min at 98 °C. After cooling to room temperature, the resulting mixture was treated with 30% H$_2$O$_2$ solution (7 mL). The mixture was washed with HCl and H$_2$O respectively, followed by centrifugation and drying, graphene oxide was thus obtained (0.38 g).
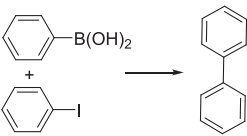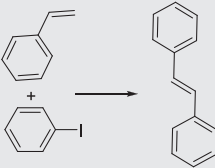
3.3 | Synthesis of GO-CPTMS

The prepared GO (0.5 gr) was dispersed in 10.0 mL of toluene by ultrasonic treatment for 15 min. Then, CPTMS (0.8 mL) was added to the mixture. At reflux temperature, the resulting mixture was stirred for 24 hr. Finally, after air cooling, the mixture was centrifuged and the solid obtained on the filter was dried at room temperature.

3.4 | Preparation of HPTPy

To a solution of 4-anisaldehyde (0.12 mL, 1 mmol) in ethanol (5 mL) was added 2-acetylpyridine (0.22 ml, 2 mmol) and potassium hydroxide (0.15 g, 2 mmol). After stirring

TABLE 7 Comparison of the efficiency of the synthesized catalyst with some previously reported catalysts in cross-coupling reactions

Entry	Reaction	Conditions	Pd (mol%)	Time	Yield^a (%)
1		GO/NHC-Pd, Na$_3$PO$_4$.12H$_2$O, H$_2$O, 100 °C [65]	1	6 h	91.6
2		GO–NHC–Pd, Cs$_2$CO$_3$, DMF/H$_2$O, 50 °C[66]	1	1 h	98
3		GO-NH$_2$-Pd, K$_2$CO$_3$, EtOH/H$_2$O, 60 °C [67]	1	30 min	87
4		GO–2 N–Pd (II), K$_2$CO$_3$, EtOH, 80 °C [68]	0.5	30 min	100
5		Pd-slGO-60, K$_2$CO$_3$, EtOH, rt [69]	0.01	2 h	99
6		NHC-Pd/GO- Ionic Liquid, K$_2$CO$_3$, EtOH/H$_2$O, 60 °C [70]	0.1	2.5 h	98
7		GO-CPTMS@Pd-TKHPP, K$_2$CO$_3$, EtOH/H$_2$O, 80 °C[26]	10	15 min	99
8		This work	1.38	3 h	95
9		GO/NHC-Pd, K$_2$CO$_3$, H$_2$O, 120 °C[65]	1	12 h	80
10		Pd/Metformin/GO, Et$_3$N, DMF, 110 °C[71]	0.1	1 h	96
11		TRGO-NPy-Pd, Na$_2$CO$_3$, DMF, 140 °C[72]	0.3	5 h	97
12		ERGO-Pd, Et$_3$N, DMF, 120 °C[73]	0.3	2 h	91
13		Pd/GO, C$_{16}$TAB, 50% aq. EG, 80 °C[74]	0.09	24 h	96
14		GO-PMMA-Pd, H$_2$O, K$_2$CO$_3$,TBAB, 100 °C[75]	0.2	4 h	80
15		GO-CPTMS@Pd-TKHPP, K$_2$CO$_3$, DMF, 120 °C[26]	10	20 min	95
16		This work	1.38	4 h	95

^{a}Isolated yields.

at room temperature, to the mixture was added ammonium hydroxide (2.9 mL, 2.5 mmol) and stirring was continued for 8 hr. The resulting precipitate was filtered and recrystallized from ethanol to produce 4′-(4-methoxyphenyl)-2,2′:6′,2″-terpyridine as white crystals in 85% yield (Found: Mp = 156 °C).[35] Then 4′-(4-methoxyphenyl)- 2,2′:6′,2″-terpyridine (0.676 g, 2 mmol) was treated with 30% HBr in acetic acid (4 mL) at reflux conditions for 4 hr. The mixture was allowed to cool to room temperature. The resultant solution was then basified to $pH = 10$ by adding aqueous NaOH (20%) dropwise and extracted repeatedly with CH_2Cl_2. The pH of the alkaline solution was then lowered with HCl (20%). The addition of HCl converts the soluble salt back into the water-insoluble HPTPy as white crystals. The precipitated product was then filtered and collected in 60% yield (Found: Mp = 290 °C,[35] IR (KBr): 3385, 1594, 1526, 1460, 1175, 779 and 734 cm^{-1}. ^{1}H NMR (250 MHz, DMSO-d$_6$): δ = 9.03–9.06 (d, J = 7.75 Hz, 2H), 8.93 (s, 2H), 8.78 (s, 2H), 8.45–8.50 (t, 2H), 7.91 (s, 4H), 6.93–6.97 (d, J = 7.75 Hz, 2H), 4.47 (br. s, OH).[13] ^{13}C NMR (250 MHz, DMSO-d$_6$): δ = 160.21, 151.23, 150.35, 146.08, 143.50, 132.12, 129.33, 128.40, 127.00, 124.17, 120.01, 116.45. MS: 327, 326, 325(M$^+$), 324, 308, 297, 296, 248, 247, 221, 220, 219, 218, 190, 163, 78, 51.

3.5 | Synthesis of GO-CPTMS@TPy

The GO-CPTMS (0.1 gr) was dispersed in DMF (10 mL) and HPTPy (0.0325 g, 0.1 mmol), Na_2CO_3 (0.04 g, 0.4 mmol) and KI (0.05 g, 0.3 mmol) were added. The mixture was heated to reflux for 24 hr. The excess of HPTPy and sodium and potassium salts were removed by washing three times with EtOH and deionized H_2O, respectively. Eventually, the obtained GO-CPTMS@TPy was separated and dried at 50 °C.

3.6 | Preparation of TPy-C$_6$H$_4$-TPy

A mixture of 2-acetylpyridine (0.9 mL, 8.3 mmol), benzene-1,4-dicarbaldehyde (0.27 g, 2.1 mmol) and 15% aq. KOH (2.9 mL) in ethanol (20 mL) was stirred. After stirring at room temperature, NH_4OH (29 mL) was added to the solution and vigorous stirring was maintained at refluxing temperature for 48 hr. After this time, the resulting mixture was cooled, and the precipitate collected by filtration, washed with ethanol and water and dried. The 1,4-bis(2,2′:6′,2″-terpyridin-4′-yl)benzene (TPy-C$_6$H$_4$-TPy) was obtained in 50% isolated yield. (Found: Mp > 320 °C,[38] IR (KBr): 1588, 1560, 1469, 1388, 785 and 734 cm^{-1}. ^{1}H NMR (250 MHz, (CDCl$_3$): δ = 8.69–8.81 (m, 12H), 7.99–8.07 (m, 8H), 7.38 (s, 4H).

3.7 | Synthesis of (1,4-C$_6$H$_4$)(GO-CPTMS@HPTPy-Pd-TPy)$_2$

0.1. g of GO-CPTMS@TPy was sonicated in 5 mL ethanol for 10 min. To the resulting mixture Pd (Cl)$_2$ (0.03 gr, 0.169 mmol) and TPy-C$_6$H$_4$-TPy (0.054 gr, 0.1 mmol) were added and refluxed for 24 hr. Then, the mixture was filtered and the solid catalyst was washed with EtOH and deionized water to remove the excess TPy-C$_6$H$_4$-TPy and PdCl$_2$ and dried under vacuum for 24 hr. ICP showed 0.138 mmol of palladium is loaded on the 0.1 gr of (1,4-C$_6$H$_4$) (GO-CPTMS@HPTPy-Pd-TPy)$_2$ (14.7 wt%).

3.8 | General procedure for Suzuki–Miyaura cross- coupling reactions

The catalyst (0.01 gr, 1.38 mol%) was dispersed in a mixture of EtOH/H$_2$O (2/1). ArX (1.2 mmol), ArB (OH)$_2$ (1 mmol) and K$_2$CO$_3$ (1.5 mmol) were added consecutively. The mixture was then stirred in an 80 °C oil bath for an appropriate reaction time. The progress of the reaction was monitored by TLC. After completion of the reaction, ethyl acetate (10 mL) was added into the reaction mixture, the catalyst was separated by centrifugation and the organic solvent was evaporated to obtain a biaryl product.

3.9 | General procedure for Mizoroki—Heck cross- coupling reactions

To a flask, a mixture of the catalyst (0.01 gr, 1.38 mol%), aryl halide (1 mmol), styrene (1.2 mmol) and Et$_3$N (3 mmol) was added and heated at 100 °C under solvent-free conditions for a specific time. When the reaction was completed as indicated by TLC, ethylacetate (10 mL) was added to the flask. The catalyst was separated by centrifugation. Water (3 × 15 mL) was added to the ethylacetate phase and decanted. After evaporation of the solvent, the resulting crude products were product was purified in hexane–ethylacetate giving the pure products in high to excellent yields.

3.10 | General procedure for arylation of amines and phenols

A mixture of aryl halide (1 mmol), amine or phenol (1 mmol), K$_2$CO$_3$ (3 mmol) and the Pd nanocatalyst (0.01 gr, 1.38 mol%) in DMF (3.0 mL) was stirred at 100 °C (oil bath temperature). After completion of the

reaction, which was monitored by TLC, ethylacetate (10 mL) was added to the mixture reaction. The catalyst was separated by centrifugation. Water (15 mL) was added to the ethylacetate phase and decanted. After evaporation of the solvent, the resulting crude products were product was purified in ethanol–water giving the pure products in high to excellent yields.

4 | CONCLUSIONS

In summary, we have successfully prepared and characterized GO supported palladium nanoparticles as a highly efficient and general nanocatalyst that is produced by an inexpensive and simple method. As expected, this nanocatalyst exhibited excellent activity in the cross-coupling reactions. Ultimately, we believe that this work provides directions for future rational design and production of nanocatalysts and heterogenization of metal catalysts. Further studies will be devoted to extend the development of this class of nanocatalysts in order to improve their catalytic efficiency in cross-coupling reactions.

ORCID

Kiumars Bahrami https://orcid.org/0000-0001-9229-0890

REFERENCES

[1] P. Devendar, R. Qu, W. Kang, B. He, G. Yang, *J. Agric. Food Chem.* **2018**, *66*, 8914.

[2] G. C. Fortman, S. P. Nolan, *Chem. Soc. Rev.* **2011**, *40*, 5151.

[3] J.-P. Corbet, G. Mignani, *Chem. Rev.* **2006**, *106*, 2651.

[4] N. Yasuda, *J. Organomet. Chem.* **2002**, *653*, 279.

[5] D. Sierra, G. Brito, M. Fuentealba, A. H. Klahn, *Inorg. Chem. Commun.* **2018**, *88*, 30.

[6] P. Ruiz-Castillo, S. L. Buchwald, *Chem. Rev.* **2016**, *116*, 12564.

[7] D. Lopez-Tejedor, B. Rivas, J. M. Palomo, *Molecules* **2018**, *23*, 2358.

[8] D. H. Howe, R. M. McDaniel, A. J. D. Magenau, *Macromolecules* **2017**, *50*, 8010.

[9] S. Chu, N. Münster, T. Balan, M. D. Smith, *Angew. Chem. Int. Ed.* **2016**, *55*, 14306.

[10] S. N. Jadhav, A. S. Kumbhar, C. V. Rode, R. S. Salunkhe, *Green Chem.* **2016**, *18*, 1898.

[11] C. C. Johansson Seechurn, M. O. Kitching, T. J. Colacot, V. Snieckus, *Angew. Chem. Int. Ed.* **2012**, *51*, 5062.

[12] J. M. Brown, *Angew. Chem. Int. Ed.* **2015**, *54*, 5003.

[13] M. Gholinejad, F. Hamed, P. Biji, *Dalton Trans.* **2015**, *44*, 14293.

[14] V. Polshettiwar, A. Molnár, *Tetrahedron* **2007**, *63*, 6949.

[15] L. Yin, J. Liebscher, *Chem. Rev.* **2007**, *107*, 133.

[16] M. Lamblin, L. Nassar-Hardy, J. C. Hierso, E. Fouquet, F. X. Felpin, *Adv. Synth. Catal.* **2010**, *352*, 33.

[17] M. Mora, C. Jimenez-Sanchidrian, J. Rafael Ruiz, *Curr. Org. Chem.* **2012**, *16*, 1128.

[18] L. Djakovitch, F. X. Felpin, *ChemCatChem* **2014**, *6*, 2175.

[19] T. Baran, I. Sargın, M. Kaya, P. Mulerčikas, S. Kazlauskaitė, A. Mentes, *Chem. Eng. J.* **2018**, *331*, 102.

[20] R. Jin, *Nanotechnol. Rev.* **2012**, *1*, 31.

[21] V. Polshettiwar, R. S. Varma, *Green Chem.* **2010**, *12*, 743.

[22] X. Chen, G. Wu, J. Chen, X. Chen, Z. Xie, X. Wang, *J. Am. Chem. Soc.* **2011**, *133*, 3693.

[23] L. Wang, Y. Wang, X. Wang, X. Feng, X. Ye, J. Fu, *Nanomaterials* **2018**, *8*, 113.

[24] D. Astruc, F. Lu, J. R. Aranzaes, *Angew. Chem. Int. Ed.* **2005**, *44*, 7852.

[25] A. M. Dimiev, J. M. Tour, *ACS Nano* **2014**, *8*, 3060.

[26] K. Bahrami, S. N. Kamrani, *Appl. Organomet. Chem.* **2018**, *32*, 4102.

[27] D. C. Marcano, D. V. Kosynkin, J. M. Berlin, A. Sinitskii, Z. Sun, A. Slesarev, L. B. Alemany, W. Lu, J. M. Tour, *ACS Nano* **2010**, *4*, 4806.

[28] J. Paredes, S. Villar-Rodil, A. Martínez-Alonso, J. Tascon, *Langmuir* **2008**, *24*, 10560.

[29] F. Li, J. Zhao, Z. Chen, *J. Phys. Chem. C* **2012**, *16*, 2507.

[30] D. Chen, H. Feng, J. Li, *Chem. Rev.* **2012**, *112*, 6027.

[31] S. Ray, *Applications of graphene and graphene-oxide based nanomaterials*, William Andrew, USA, **2015**.

[32] G. T. Morgan, F. H. Burstall, *J. Chem. Soc.* **1932**, 20.

[33] D. Dong, Z. Li, D. Liu, N. Yu, H. Zhao, H. Chen, J. Liua, D. Liu, *New J. Chem.* **2018**, *42*, 9317.

[34] C. Zanardi, B. Zanfrognini, S. Morandi, F. Terzi, L. Pigani, L. Pasquali, R. Seeber, *Electrochim. Acta* **2018**, *260*, 314.

[35] W. Spahni, G. Calzagerri, *Helv. Chim. Acta* **1984**, *67*, 450.

[36] W. S. Hummers Jr., R. E. Offeman, *J. Am. Chem. Soc.* **1958**, *80*, 1339.

[37] K. Bahrami, M. M. Khodaei, F. S. Meibodi, *Appl. Organomet. Chem.* **2017**, *31*, 3627.

[38] S. Vaduvescu, P. G. Potvin, *Eur. J. Inorg. Chem.* **2004**, *8*, 1763.

[39] C. Putta, V. Sharavath, S. Sarkara, S. Ghosh, *RSC Adv.* **2015**, *5*, 6652.

[40] C. B. Putta, S. Ghosh, *Adv. Synth. Catal.* **2011**, *353*, 1889.

[41] N. Basavegowda, K. Mishra, Y. R. Lee, *New J. Chem.* **2014**, *39*, 72.

[42] M. R. Shaik, Z. J. Q. Ali, M. Khan, M. Kuniyil, M. E. Assal, H. Z. Alkhathlan, A. Al-Warthan, M. R. H. Siddiqui, M. Khan, S. F. Adil, *Molecules* **2017**, *22*, 165.

[43] E. Ramirez, S. Jansat, K. Philippot, P. Lecante, M. Gomez, A. M. Masdeu-Bulto, B. Chaudret, *J. Organom. Chem.* **2004**, *689*, 4601.

[44] S. Sobhani, Z. Zeraatkar, F. Zarifi, *New J. Chem.* **2015**, *39*, 7076.

[45] A. Villa, D. Wang, P. Spontoni, R. Arrigo, D. S. Su, L. Pratia, *Catal. Today* **2010**, *157*, 89.

[46] U. Yilmaz, H. Kucukbay, S. T. Celikesir, M. Akkurt, O. Buyukgungor, *Turk. J. Chem.* **2013**, *37*, 721.

[47] F. Durap, O. Metin, M. Aydemir, S. Ozkar, *Appl. Organomet. Chem.* **2009**, *24*, 498.

[48] P. Kumar, G. Singh, D. Tripathi, S. L. Jain, *RSC Adv.* **2014**, *4*, 50331.

[49] Y. Y. Peng, J. Liu, X. Lei, Z. Yin, *Green Chem.* **2010**, *12*, 1072.

[50] X. Zeng, T. Zhang, Y. Qin, Z. Wei, M. Luo, *Dalton Trans.* **2009**, 8341.

[51] D. Hey, S. Orman, G. H. Williams, *J. Chem. Soc.* **1965**, 101.

[52] N. A. Bumagin, V. V. Bykov, *Tetrahedron* **1997**, *53*, 14437.

[53] H. J. Xu, Y. Q. Zhao, X. F. Zhou, *J. Org. Chem.* **2011**, *76*, 8036.

[54] N. Iranpoor, H. Firouzabadi, A. Tarassoli, M. Fereidoonnezhad, *Tetrahedron* **2010**, *66*, 2415.

[55] F. M. Beringer, A. Brierley, M. Drexler, E. M. Gindler, C. C. Lumpkin, *J. Am. Chem. Soc.* **1953**, *75*, 2708.

[56] L. Hayward, R. Kitchen, D. Livingstone, *Can. J. Chem.* **1962**, *40*, 434.

[57] H. Zhang, Q. Cai, D. Ma, *J. Org. Chem.* **2005**, *70*, 5164.

[58] W. W. Leake, R. Levine, *J. Am. Chem. Soc.* **1959**, *81*, 1169.

[59] H. J. Cristau, P. P. Cellier, S. Hamada, J. F. Spindler, M. Taillefer, *Org. Lett.* **2004**, *6*, 913.

[60] H. Xu, F. Ye, H. L. Dai, *Chin. J. Chem.* **2008**, *26*, 1465.

[61] H. M. Colquhoun, D. F. Lewis, *Polymer* **1988**, *29*, 1902.

[62] R. Begunov, A. Valyaeva, V. Belyaev, N. Dobretsova, *Russ. Chem. Bull.* **2015**, *64*, 1971.

[63] J. S. Sawyer, E. A. Schmittling, J. A. Palkowitz, W. J. Smith, *J. Org. Chem.* **1998**, *63*, 6338.

[64] H. Keipoura, A. Hosseini, A. Afsari, R. Oladee, M. A. Khalilzadeh, T. Ollevier, *Can. J. Chem.* **2016**, *94*, 95.

[65] S. Kim, H. Cho, D. Shin, S. Lee, *Tetrahedron Lett.* **2017**, *58*, 2421.

[66] J. H. Park, F. Raza, S. Jeon, H. Kim, T. W. Kang, D. B. Yim, J. Kim, *Tetrahedron Lett.* **2014**, *55*, 3426.

[67] N. Shang, C. Feng, H. Zhang, S. Gao, R. Tang, C. Wang, Z. Wang, *Cat. Com.* **2013**, *40*, 111.

[68] C. Bai, Q. Zhao, Y. Li, G. Zhang, F. Zhang, X. Fan, *Catal. Lett.* **2014**, *144*, 1617.

[69] S. Yamamoto, H. Kinoshita, H. Hashimoto, Y. Nishina, *Nanoscale* **2014**, *6*, 6501.

[70] A. S. K. Movahed, R. Esmatpoursalmani, A. Bazgir, *RSC Adv.* **2014**, *4*, 14586.

[71] H. Veisi, N. Mirzaee, *Appl. Organomet. Chem.* **2018**, *23*, e4067.

[72] L. Fernández-García, M. Blanco, C. Blanco, P. Álvarez, M. Granda, R. Santamaría, R. Menéndez, *J. Mol. Catal. A: Chem* **2016**, *416*, 140.

[73] S. S. Shendage, J. M. Nagarkar, *Colloids Interface Sci Commun* **2014**, *1*, 47.

[74] A. Saito, S. Yamamoto, Y. Nishina, *RSC Adv.* **2014**, *4*, 59835.

[75] P. Basak, P. Ghosh, *Synth. Commun.* **2018**, *48*, 1.

SUPPORTING INFORMATION

Additional supporting information may be found online in the Supporting Information section at the end of the article.